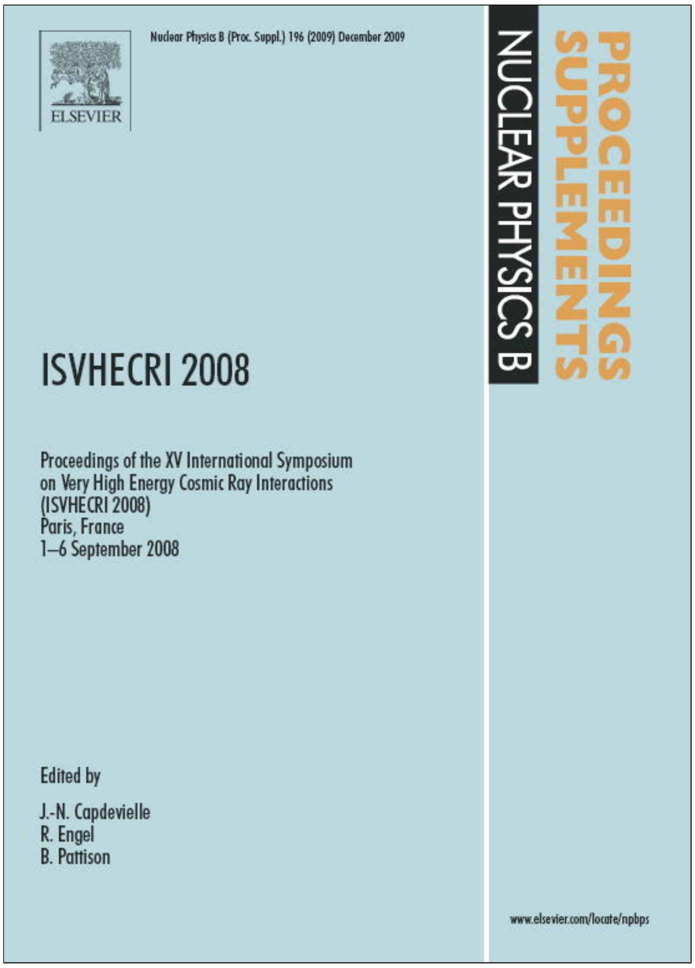
Nuclear Physics B (Proc. Suppl.) 196 (2009) December 2009
ELSEVIER
NUCLEAR PHYSICS B
PROCEEDINGS SUPPLEMENTS
ISVHECRI 2008
Proceedings of the XV International Symposium on Very High Energy Cosmic Ray Interactions (ISVHECRI 2008) Paris, France 1–6 September 2008
Edited by
J.-N. Capdevielle
R. Engel
B. Pattison
www.elsevier.com/locate/npbps

Available online at www.sciencedirect.com
ScienceDirect
ELSEVIER
Nuclear Physics B (Proc. Suppl.) 196 (2009) 173–178
NUCLEAR PHYSICS B
PROCEEDINGS SUPPLEMENTS
www.elsevier.com/locate/npbps

Does the GAMMA experiment detect the polar cap component at energies 70-80 PeV?

R.M. Martirosov[a] , A.P. Garyaka[a], S.V. Ter-Antonyan[b], A.D. Erlykin[c], N.M. Nikolskaya[c], Y.A. Gallant[d], L.W. Jones[e], and J. Procureur[f]

[a]Yerevan Physics Institute, 2 Alikhanyan Br. Str., 036 Yerevan, Armenia

[b]Department of Physics, Southern University, Baton Rouge, USA

[c]P.N.Lebedev Physical Institute, Moscow, Russia

[d]LPTA, Universite Montpellier II, CNRS/IN2P3, Montpellier, France

[e]Department of Physics, University of Michigan, USA

[f]Centre d'Etudes Nucleaires de Bordeaux-Gradignan, Gradignan, France

The all-particle energy spectrum of the primary cosmic rays at energies 1-200 PeV has been obtained on the basis of the GAMMA experimental data using the event-by-event method of the primary energy evaluation from the measured N_{ch}, N_μ and shower age (s) parameters. The energy estimation method was developed using the CORSIKA simulation code in the frames of the SIBYLL interaction model taking into account the response of the GAMMA detectors and the reconstruction uncertainties of the EAS parameters. The observed 'bump' at $\sim 7.4 \cdot 10^7$ GeV can be described by a two-component model of primary cosmic ray origin.

1. Introduction

A search of the fine structure around the knee in the primary energy spectrum is one of the main interesting problems of the very-high energy cosmic rays [1]. It is well known that the behavior of the all-particle energy spectrum above the knee is not smooth. There are visible irregularities, especially at 10-100 PeV. Irregularities of the energy spectrum in this region were observed a long time ago. They can be seen from the energy spectrum obtained more than 20 years ago in the AKENO experiment [2]. Some indications of the observed bump are also seen in the KASCADE-Grande [3], TUNKA [4], and TIBET-III [5] experiments but with larger statistical uncertainties at a level of $1.5 - 2.0$ standard deviations. At the same time the large statistical errors did not allow us to discuss the reasons for these irregularities.

It is necessary to underline that many experimental results on the study of extensive air showers (EAS) indicate that some of the characteristics of EAS behind the knee are changing, in particular the behavior of the age parameter and muon component characteristics. Based on these indications, additional investigations into the fine structure of the primary energy spectrum at $(1 - 10) \cdot 10^7$ GeV have a special interest.

One way to obtain the primary energy spectra is the method based on an event-by-event evaluation of the primary energy of the detected EAS with parameters $\mathbf{q} \equiv q(N_e, N_\mu, N_h, s, \theta)$, using a parametric estimator previously determined on the basis of shower simulations in the framework of a given model of EAS development. In this work applying a new event-by-event parametric energy evaluation $E = f(q)$ the all-particle energy spectrum in the knee region is derived on the basis of the GAMMA EAS array [6,7] experimental data and a simulated EAS database obtained using the SIBYLL [8] interaction model.

2. GAMMA experiment

The GAMMA installation [6,7,11] is a ground based array of 33 surface detector stations and

doi:10.1016/j.nuclphysbps.2009.09.031

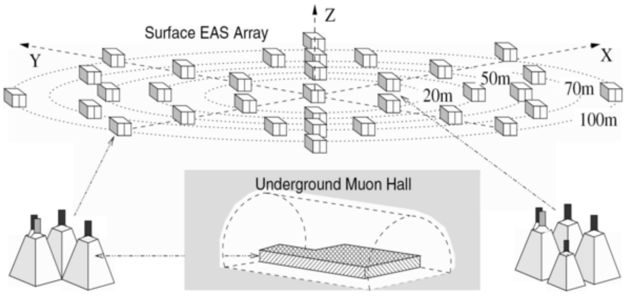

Figure 1. Layout of the GAMMA installation

150 underground muon detectors, located on the south side of Mount Aragats in Armenia. The elevation of the GAMMA facility is 3200 m above sea level, corresponding to 700 g/cm^2 of atmospheric depth. A diagrammatic layout of the array is shown in Fig. 1. The surface stations of the EAS array are arranged in 5 concentric circles of $\sim$ 20, 28, 50, 70 and 100 m radii, and each station contains 3 plastic scintillation detectors with dimensions of $1 \times 1 \times 0.05$ m^3. Each of the central 9 stations contains an additional (the 4th) small scintillator with dimensions of $0.3 \times 0.3 \times 0.05$ m^3 for high particle density ($\gg 10^2$ particles/m^2) measurements.

A photomultiplier tube is placed on top of the aluminum casing covering each scintillator. One of the three detectors of each station is viewed by two photomultipliers, one of which is designed for fast timing measurements.

150 underground muon detectors ('muon carpet') are compactly arranged in the underground hall under 2.3 kg/cm^2 of concrete and rock. The scintillator dimensions, casings and photomultipliers are the same as in the EAS surface detectors.

The shower size thresholds of the 100% shower detection efficiency are equal to $N_{ch} = 3 \cdot 10^5$ and $N_{ch} = 5 \cdot 10^5$ at the EAS core location within R< 25 m and R< 50 m respectively.

The time delay is estimated by the pair-delay method [9] to give a time resolution of about 4-5 ns. The EAS detection efficiency (P_d) and corresponding shower parameter reconstruction accuracies are equal to: $P_d = 100\%$, $\Delta\theta \simeq 1.5°$, $\Delta N_{ch}/N_{ch} \simeq 0.1$, $\Delta s \simeq 0.05$, Δx and $\Delta y \simeq 0.7 - 1$ m. The reconstruction accuracies of the truncated muon shower sizes for $R_\mu < 50$ m from the shower core are equal to $\Delta N_\mu/N_\mu \simeq 0.2-0.35$ at $N_\mu \simeq 10^5 - 10^3$ respectively.

3. All-particle energy spectrum

The EAS data set analyzed in this paper has been obtained for $5.63 \cdot 10^7$ sec of live run time of the GAMMA facility, from 2004 to 2006. Showers analyzed were selected with the following criteria: $N_{ch} > 5 \cdot 10^5$, $R < 50$ m, $\theta < 45°$, $0.3 < s < 1.6$, $\chi^2(N_{ch})/n < 3$ and $\chi^2(N_\mu)/n < 3$ (where n is the number of scintillators with non-zero signal), yielding a total data set of $\sim 7 \cdot 10^5$ selected showers. The selected measurement range provided the 100% EAS detection efficiency and similar conditions for the reconstruction of showers produced by primary nuclei H, He,... , Fe with energies $3 < E < 200 - 300$ PeV.

Using the unbiased (< 5%) event-by-event method of primary energy evaluation, we obtained the all-particle energy spectrum. Results are presented in Fig. 2 (filled circle symbols, GAMMA07) in comparison with the same spectra obtained by the EAS inverse approach (line with shaded area, GAMMA06) from [3,6] and our preliminary results (point-circle symbols, GAMMA05) obtained using the event-by-event method with the shower core selection criteria $R < 25\ m$ and $\theta < 30°$ [10].

It follows from our preliminary data, that the all-particle energy spectrum derived by event-by-event analysis with the multi-parametric energy estimator depends only slightly on the interaction model (QGSJET01 [12] or SIBYLL2.1 [8]) and thereby, the accuracies of the obtained spectra are mainly determined by the sum of the statistical and methodical errors presented in Fig. 2 by the dark shaded area.

The shower size detection threshold effects distort the all-particle spectrum in the range of $E < 2 - 2.5$ PeV depending on the interaction model and determine the lower limit $E_{\min} = 3$ PeV of the energy spectrum in Fig. 2 whereas the upper limit of the spectrum $E_{\max} \simeq 200 - 300$ PeV is

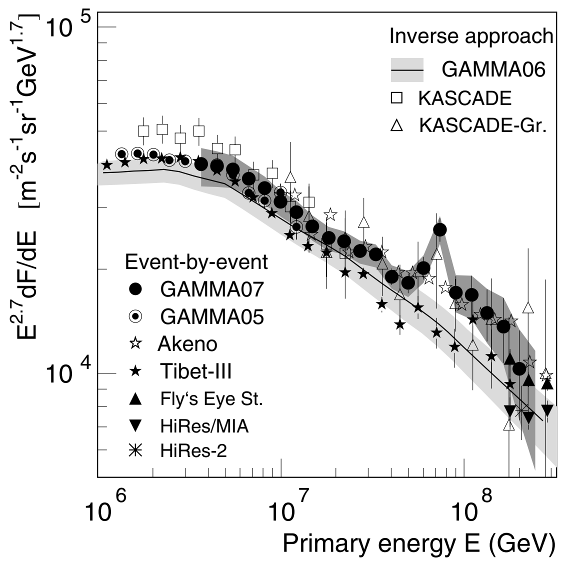

Figure 2. The all-particle energy spectrum compared with the results of EAS inverse approach [3,6] and our preliminary data [10]. The AKENO, Tibet-III, Fly's Eye Stereo, Hires/MIA and Hires-2 data were taken from [2,18–21] respectively.

determined by the saturation of our shower detectors which begins to be significant at $E_p > 200$ PeV and $E_{Fe} > 400$ PeV for primary proton and Fe nuclei. The range of minimal methodical errors and biases is 10-100 PeV, where about 13% and 10% accuracies were attained for primary H and Fe nuclei respectively.

The obtained energy spectrum agrees within errors with the KASCADE [3] AKENO [2] and Tibet-III [5] data both in the slope and in the absolute intensity practically over the whole measurement range. However, our statistical and methodical errors are less than in those experiments.

Looking at the experimental points we can unambiguously point out the existence of an irregularity in the spectrum at the energy of $60 - 80$ PeV. The energy estimator has minimal biases ($\sim 4 - 5\%$) and errors ($\sim 0.09 - 0.12$) at this energy. Within these errors the obtained bump is apparently real. If we fit all our other points in the 5-200 PeV energy range by a smooth power-law spectrum, the bin at 74 PeV exceeds this smooth spectrum by 4.0 standard deviations. The exact value for the significance of the bump depends somewhat on the energy range chosen to adjust the reference straight line in Fig. 2, but it lies in the range 3.5-4.5 σ.

We conservatively included the systematic errors in this estimate, although they are not independent in the nearby points but correlated: the possible overestimation of the energy in one point cannot be followed by an underestimation in the neighboring point if their energies are relatively close to each other. Systematic errors can slightly change the general slope of the spectrum but cannot imitate the fine structure and the existence of the bump.

It is necessary to note again that some indications of the mentioned bump are seen also in the KASCADE-Grande [3], TUNKA [4] and TIBET [5] data but with larger statistical uncertainties. Moreover, the locations of the bump in different experiments agree well with each other and with an expected knee energy for Fe-like primary nuclei according to the rigidity-dependent knee hypothesis [6]. However, the observed width ($\sim$ 20% in energy) and height of the bump in the energy range 60-80 PeV, exceeds by a factor of ~ 1.5 (~ 4 standard deviations) the best fit straight line fitting all points above 5 PeV in Fig. 2, are difficult to describe in the framework of the conventional model of cosmic ray origin [13].

The detected EAS charged particle (N_{ch}) and muon size (N_μ) spectra [6] independently indicate the existence of this bump at the obtained energies and as it follows from the behavior of the shower age parameter versus shower size [6], the bump at energy 70-80 PeV is likely formed completely from Fe nuclei.

4. Possible origin of irregularities

Irregularities of the all-particle energy spectrum in the knee region are observed in practically all measurements [2–5,7] and are explained by both the rigidity-dependent knee hypothesis and the contribution of pulsars in the Galactic cosmic ray flux [14–16]. Two of these approaches

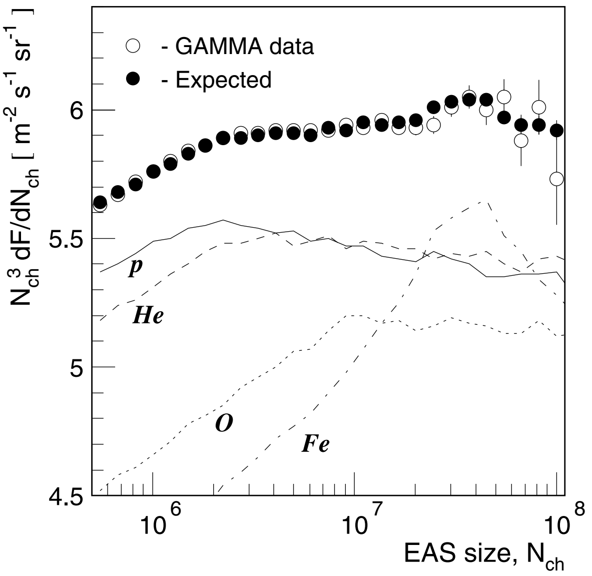

Figure 3. EAS size spectra detected by the GAMMA facility (empty symbols) and the corresponding expected spectra (filled symbols) computed in the framework of the SIBYLL2.1 interaction model and 2-component parametrization of the primary spectra. The lines correspond to the expected size spectra computed for each primary nuclei.

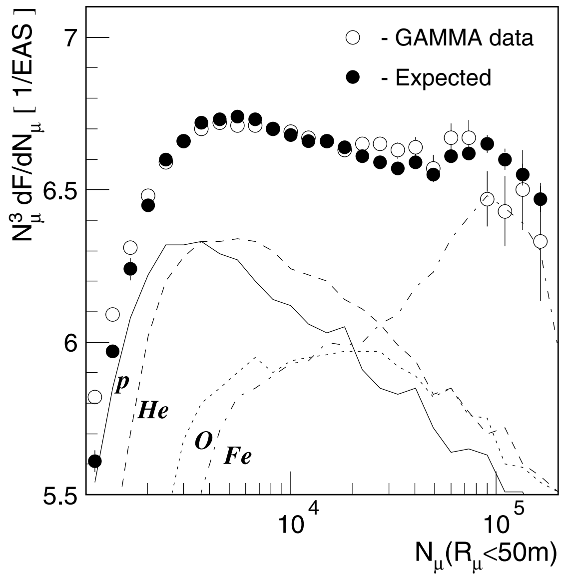

Figure 4. The same as Fig. 3 for truncated EAS muon size spectra.

approximately describe the all-particle spectrum in the $(1-100)\cdot 10^6$ GeV energy region. However, the observed bump in Fig. 2 at $\sim 7.4\cdot 10^7$ GeV directly indicates the presence of an additional component in the primary nuclei flux and displays a very flat ($\gamma_p \sim 0-2$) energy spectrum before a cut-off energy $E_c \simeq 8\cdot 10^7$ GeV.

It is known [6] that rigidity-dependent primary energy spectra can not describe quantitatively the phenomenon of ageing of EAS at energies $(5-10)\cdot 10^7$ GeV that was observed in mountain-altitude experiments [9,17]. It is reasonable to assume that an additional flux of heavy nuclei (Fe-like) is responsible for the bump at these energies. Besides, the sharpness of the bump (Fig. 2) points to a local origin of this flux from compact objects (pulsars) [15,16].

To test this hypothesis we used the parameterized inverse approach [6] on the basis of the GAMMA facility EAS database and the hypothesis of a two-component origin of cosmic ray flux for EAS size spectra (Fig. 3) and for truncated muon size spectra (Fig. 4). Details of the testing are described in [7]. The folded (expected) shower spectra (filled symbols in Figs. 3, 4) were computed on the basis of parametrization and the CORSIKA EAS simulated data set [6] for the A $\equiv$ H, He, O and Fe primary nuclei. The computation method was exactly the same as used in the combined approximation analysis [6]. The initial values of spectral parameters for the Galactic component were also taken from [6]. In Figs. 3, 4 we also present the derived expected elemental shower spectra (lines) for primary H, He, O and Fe nuclei respectively.

The resulting expected energy spectra $F_A(E)$ for the Galactic H, He, O and Fe nuclei (thin lines) along with the all-particle spectrum $\sum_A F_A(E)$ (bold line with shaded area) are shown in Fig. 5. The thick dash-dotted line cor-

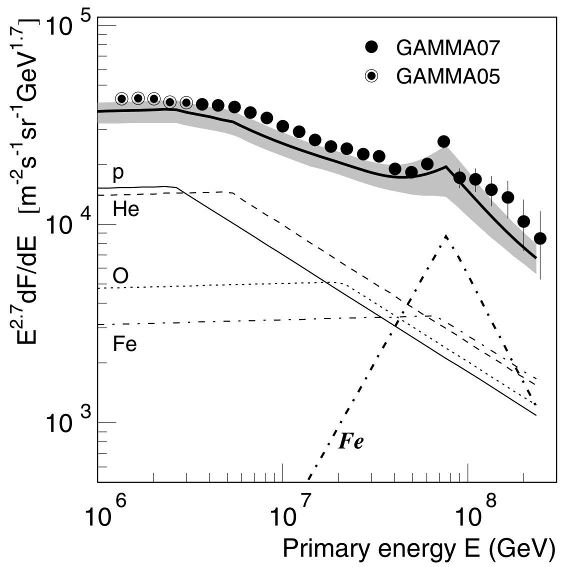

Figure 5. The all-particle primary energy spectrum (symbols) and expected energy spectra (lines and shaded area) derived from the EAS inverse problem solution for p,He,O and Fe primary nuclei using 2-component parametrization. The thin lines are the energy spectra of Galactic H,He,O and Fe components. The thick dash-dotted line is an additional Fe component from compact objects.

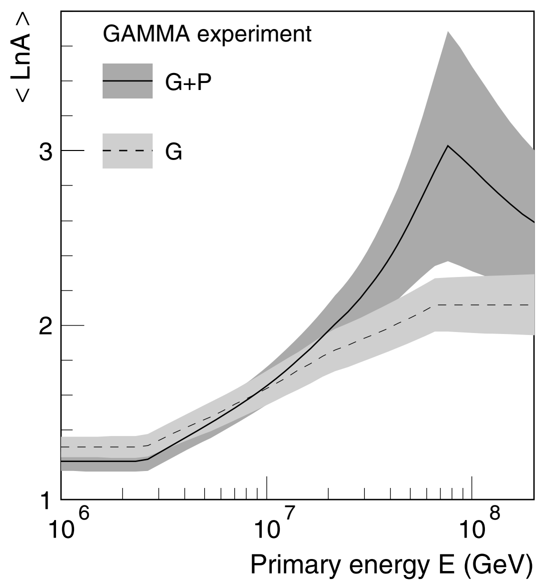

Figure 6. The average logarithm primary nuclei mass number derived from the rigidity-dependent primary energy spectra [6] (dashed line) and the 2-component model prediction taking into account an additional pulsar component (solid line).

responds to the derived energy spectra for the additional Fe component. The all-particle energy spectrum obtained on the basis of the GAMMA EAS data and event-by-event multi-parametric energy evaluation method are also shown in Fig. 5 (symbols).

It is seen, that the shape of the 2-component all-particle spectrum (bold line with shaded area) calculated with parameters taken from the fit of EAS size spectra agrees, within the errors, with the results of the event-by-event analysis (symbols) showing the consistency of the applied spectral parametrization with the GAMMA data.

Notice that the flux of the derived additional Fe component turned out to be about $0.5 - 0.6\%$ of the total Fe flux for primary energies E>10^6 GeV. This result agrees with the expected flux of the polar cap component [14].

The dependence of the average nuclear mass number are shown in Fig. 6 for two primary nuclei flux composition models: the one-component model, where the power law energy spectra of primary nuclei have rigidity-dependent knees at particle rigidity $E_R \sim 2500$ GeV/Z [6] (the so called Galactic component, dashed line) and the two-component model (solid line). The shaded area in Fig. 6 shows the ranges of total (systematic and statistical) errors.

5. Conclusion

The all-particle energy spectrum obtained with the GAMMA experiment in the 3-200 PeV energy range indicates the existence of an irregularity ('bump') in the range 60-80 PeV. The bump can be described by a 2-component model of primary cosmic ray origin, where an additional (pulsar) Fe component are included. Although we cannot reject the stochastic nature of the bump completely, our examination of the systematic uncertainties of the applied method leads us to believe that they cannot be responsible for the observed feature. The indications from other experiments mentioned in this paper provide the argument for a further study of this interesting energy region

6. Acknowledgments

We are grateful to all our colleagues at the Moscow P N Lebedev Physical Institute and the Yerevan Physics Institute who took part in the development and exploitation of the GAMMA array. We thank Peter Biermann for fruitful discussions. This work has been partly supported by the research grant no. 090 from the Armenian Government, the RFBR grant 07-02-00491 in Russia, and the 'Hayastan' All-Armenian Fund in France.

REFERENCES

1. Erlykin A.D., Wolfendale A.W., J. Phys. G: Nucl. Part. Phys., **23** (1997) 979; Astron. and Astrophys. **350** (1999) L1; J. Phys. G: Nucl. Part. Phys. **27** (2001) 1005.
2. N. Nagano, T. Hara et al., J. Phys. G: Nucl. Part. Phys. **10** (1984) 1295.
3. M. Bruggemann et al., Proc. 20^{th} ECRS, Lisbon (2006), available from http://www.lip.pt/events/2006/ecrs/proc/ercs06-s3–77.pdf.
4. E.E. Korosteleva et al., Nucl. Phys. B (Proc.Suppl.) **165** (2007) 74.
5. M. Amenomori, X.J. Bi, D. Chen et al., arXiv:0801.1803 [hep-ex] (2008).
6. A.P. Garyaka, R.M. Martirosov, S.V. Ter-Antonyan et al., Astropart.Phys. **28/2** (2007) 169; (arXiv:0704.3200v1 [astro-ph]).
7. A.P. Garyaka, R.M. Martirosov, S.V. Ter-Antonyan et al., J. Phys. G: Nucl. Part. Phys. **38** (2008) 115201.
8. R.S. Fletcher, T.K. Gaisser, P. Lipari, T. Stanev, Phys.Rev. **D50** (1994) 5710.
9. V.V. Avakian et al., Proc. 24^{th} Intern. Cosmic Ray Conf., Rome, **1** (1995) 348.
10. S.V. Ter-Antonyan et al., 29^{th} ICRC, Pune, HE1.2, **6** (2005) 105.
11. Y.A. Gallant, A.P. Garyaka, L.W. Jones et al., Proc. 20^{th} ECRS, Lisbon (2006); available from http://www.lip.pt/events/2006/ecrs/proc/ecrs06-s3-95.pdf.
12. N.N. Kalmykov, S.S. Ostapchenko, Yad. Fiz. **56** (1993) 105 (in Russian).
13. A.M. Hillas, J. Phys. G: Nucl. Part. Phys. **31** (2005) R95
14. T. Stanev, P.L. Biermann, T.K. Gaisser, Astron. Astrophys. **274** (1993) 902.
15. A.D. Erlykin and A.W. Wolfendale, Astropart. Phys., **22/1** (2004) 47 (astro-ph/0404530).
16. .W. Bednarek, R.J. Protheroe, Astropart.Phys. **16** (2002) 397.
17. S. Miyake, N. Ito et al., Proc. 16^{th} ICRC, Kyoto, **13** (1979) 171.
18. M. Amenomori, X.J. Bi, D. Chen et al., arXiv:0801.1803 [hep-ex] (2008).
19. D.J. Bird et al., Astrophys. J. **441** (1995) 144.
20. T. Abu-Zayyad et al., Astrophys. J. **557** (2001) 557.
21. R.U. Abbassi et al., astro-ph/0208301 (2002).